

Supplementary Information:

Heterojunction α -Fe₂O₃/ZnO films with enhanced photocatalytic properties grown by aerosol-assisted chemical vapour deposition

Arreerat Jiamprasertboon^{a,b}, Andreas Kafizas^{c,d}, Michael Sachs^d, Min Ling^b, Abdullah M. Alotaibi^b, Yao Lu^e, Theeranun Siritanon^a, Ivan P. Parkin^b, Claire J. Carmalt^{b*}

^a School of Chemistry, Institute of Science, Suranaree University of Technology, 111 University Avenue, Muang, Nakhon Ratchasima, 30000, Thailand

^b Material Chemistry Centre, Department of Chemistry, University College London, 20 Gordon Street, London, WC1H 0AJ, UK

^c Department of Chemistry, Imperial College London, South Kensington, London, SW7 2AZ, United Kingdom

^d The Grantham Institute, Imperial College London, South Kensington, London, SW7 2AZ, United Kingdom

^e Department of Mechanical Engineering, University College London, London, WC1E 7JE, United Kingdom

S1. X-ray photoelectron spectroscopy (XPS)

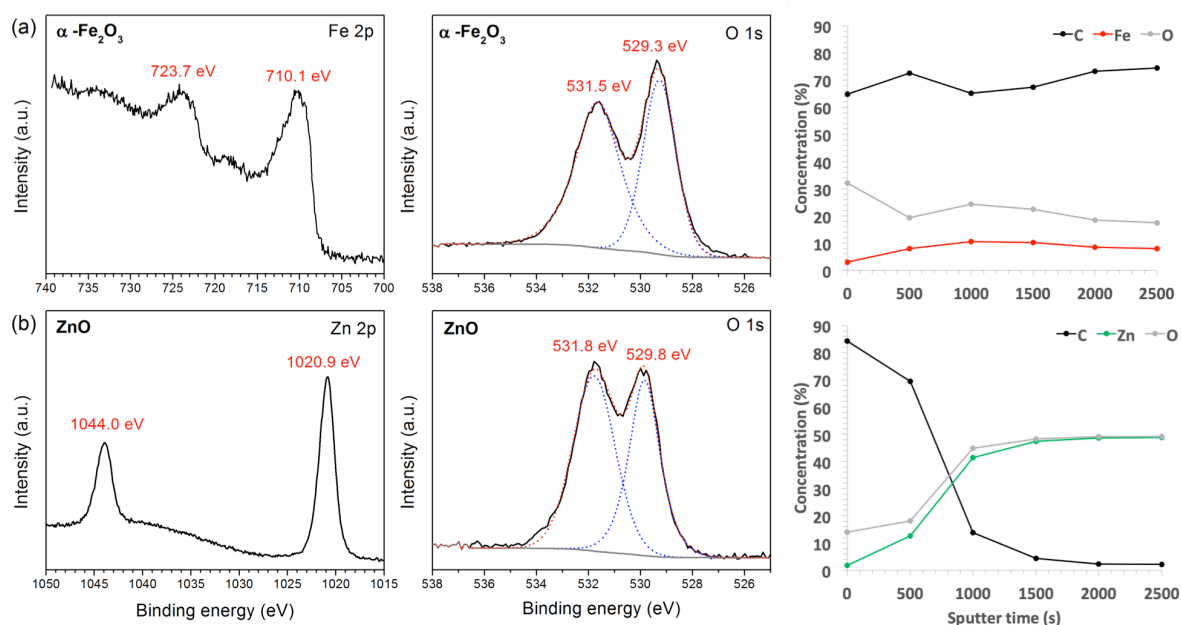


Fig. S1. The high resolution XPS spectra, and atomic compositions with sputter time, of (a) α -Fe₂O₃ and (b) ZnO films showing elemental composition.

Table S1. At.% Fe, at.% Zn and at.% O of the heterojunction film of α -Fe₂O₃/ZnO obtaining from the corrected peak areas, by using R.S.F. parameters provided by CasaXPS software, of Fe 2p_{3/2} and Zn 2p_{3/2} deconvoluted peaks.

Etching time (s)			Fe		O		at.% Fe	at.% Zn	at.% O
	R.S.F. = 28.72		R.S.F. = 16.42		R.S.F. = 2.93				
	Area Fe 2p _{3/2}	Corrected peak area	Area Fe 2p _{3/2}	Corrected peak area	Area O 2p	Corrected peak area			
0	13498.9	470.0	0	0	3859.6	1317.3	0.00	26.3	73.7
500	121833.7	4242.1	0	0	19105.3	6520.6	0.00	39.4	60.6
1,000	153154.5	5332.7	0	0	22030.8	7519.0	0.00	41.5	58.5
1,500	170069.9	5921.6	0	0	23252.3	7935.9	0.00	42.7	57.3
2,000	181817.1	6330.7	0	0	24895.1	8496.6	0.00	42.7	57.3
2,500	193375.6	6733.1	0	0	26421.7	9017.6	0.00	42.8	57.2
5,000	2804.9	148.4	39947	3698.8	20758.5	7084.8	25.3	1.0	73.7
10,000	1471.0	77.8	51241.9	4744.6	27299.9	9317.4	25.0	0.4	74.6
15,000	2226.8	117.8	54499.1	5046.2	30028.6	10248.7	24.3	0.6	75.1
20,000	11548.7	611.0	52876.9	4896.0	26997.1	9214.0	25.1	3.1	71.8
25,000	5626.0	297.7	51128.3	4734.1	30647.5	10459.9	22.6	1.4	76.0
30,000	2800.4	148.2	52585.0	4869.0	31691.3	10816.1	22.7	0.7	76.6
35,000	1831.6	96.9	52844.3	4893.0	32131.6	10966.4	22.6	0.4	77.0

S2. Energy Dispersive X-ray Spectroscopy (EDS)

Fig. S2 shows the EDS spectra and the elemental compositions of the heterojunction α -Fe₂O₃/ZnO film. By using the accelerating energy of 10 kV, Zn and O were observed while C was detected because it was used for sputtering a film surface. With higher energy, the amount of Fe was detected increasingly with the energy used from 15 kV to 20 eV.



Fig. S2. EDS spectra of the heterojunction α -Fe₂O₃/ZnO film with the use of different accelerating energy of 10 kV, 15 kV and 20 kV. The inset tables give details about weight% and atomic% of all elements detected.

S3. Transmittance and reflectance spectra

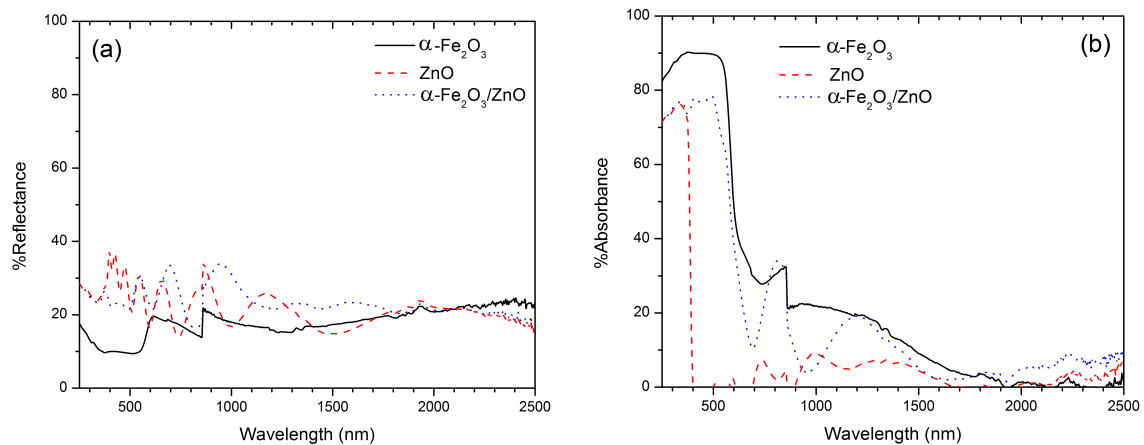


Fig. S3. (a) Reflectance and (b) absorbance UV/Vis/NIR spectra of all films synthesised: α -Fe₂O₃, ZnO and α -Fe₂O₃/ZnO. The absorbance were obtained using the formula %A = 100 - %T - %R.

S4. Band gap energies

Tauc plot [1] was utilised to determine the optical band gap energy of films. A plot displays the relationship of $(\alpha h\nu)^{1/r}$ as a function of $h\nu$, where α is absorption coefficient, h is Planck constant, ν is frequency and r is the value corresponding to the nature of transition [2]. The direct and indirect allowed transition can be expressed with the r value of 1/2 and 2, respectively. Band gap energy of α -Fe₂O₃ was reported with either direct and indirect band gap [3]. Here, the indirect band gap of 2.15 eV and the direct band gap of 2.1 eV were observed, which are similar to the report elsewhere [3]. ZnO film prepared in this work has the band gap energy of 3.3 eV, which is similar to many literatures [4,5].

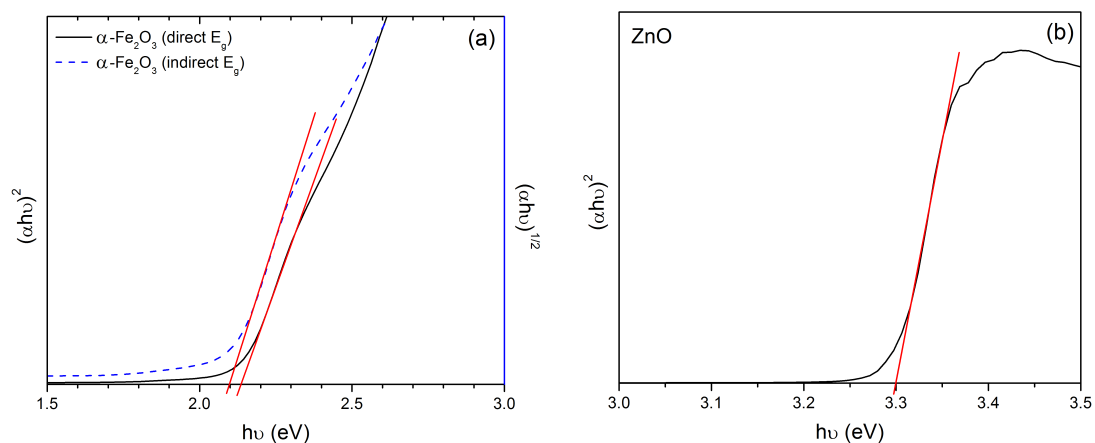


Fig. S4. Tauc plots of all single layered films. The extrapolated lines on x-axis show band gap energy (E_g). α -Fe₂O₃ has the direct band gap of 2.1 eV and the indirect band gap of 2.15 eV. ZnO has the band gap of 3.3 eV.

S5. Atomic Force Microscopy (AFM)

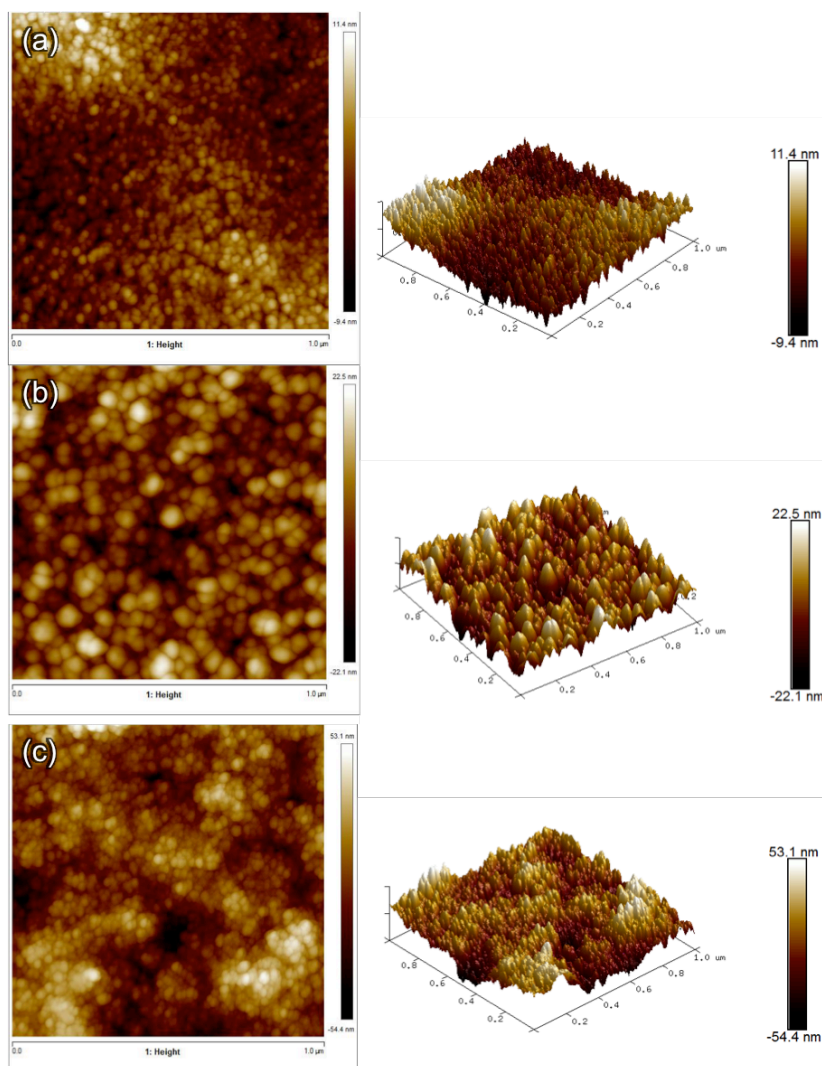


Fig. S5. AFM images of surface (left) and three-dimensional of (a) α - Fe_2O_3 film, (b) ZnO film and (c) α - $\text{Fe}_2\text{O}_3/\text{ZnO}$ film.

Table S2. Root mean squared surface roughness (R_q) and surface area obtained from AFM images of all synthesised films.

Films	R_q (nm)	Surface area (nm^2)	Projected surface area (nm^2)	Increase in surface area (factor)
α - Fe_2O_3	1.76 ± 0.04	1,031,085	1,000,000	1.03
ZnO	5.88 ± 0.19	1,105,961	1,000,000	1.11
α - $\text{Fe}_2\text{O}_3/\text{ZnO}$ heterojunction	13.4 ± 3.8	1,360,326	1,000,000	1.36

S6. Transient Absorption Spectroscopy (TAS)

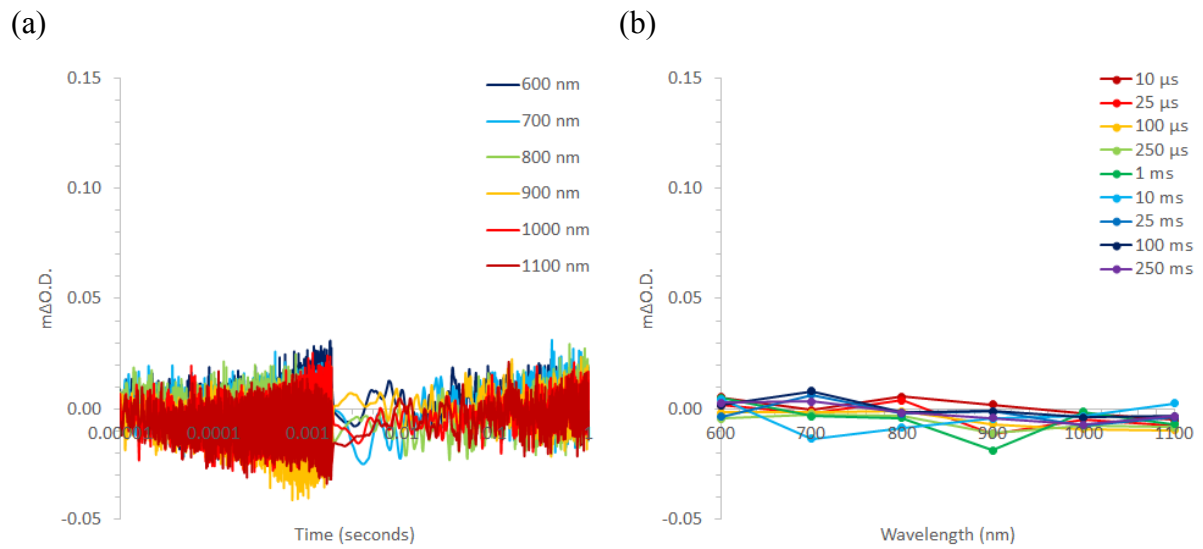


Fig. S6. (a) transient absorption decay dynamics and (b) spectral decay dynamics of a ZnO film from 10 μs after a laser pulse ($\lambda_{exc} = 355$ nm, ~ 0.5 mJ.cm $^{-2}$, 6 ns pulse width, 0.65 Hz).

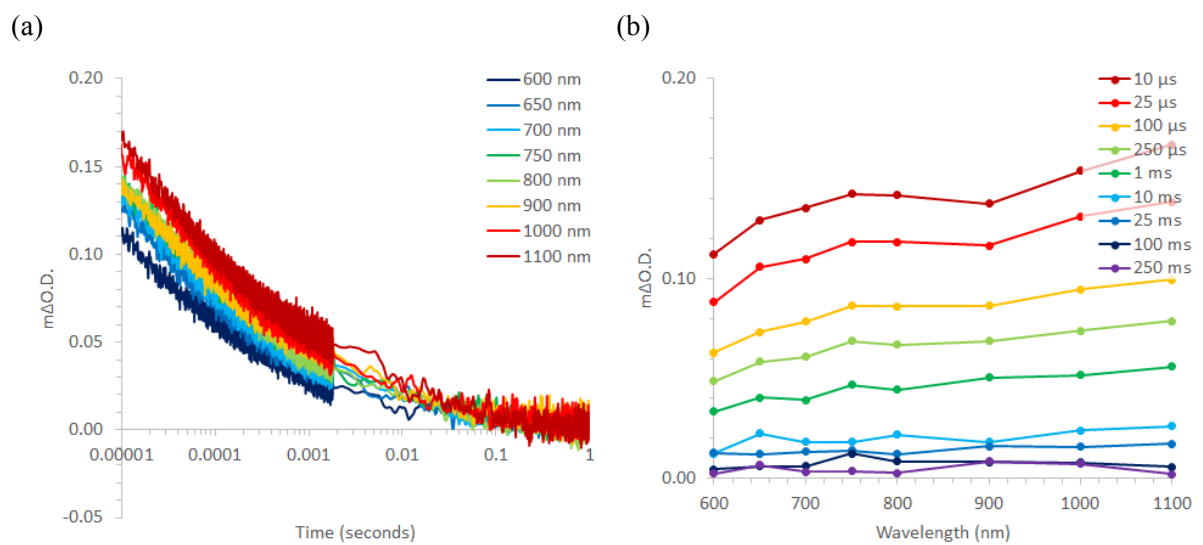


Fig. S7. (a) transient absorption decay dynamics and (b) spectral decay dynamics of an α -Fe $_2$ O $_3$ film from 10 μs after a laser pulse ($\lambda_{exc} = 355$ nm, ~ 0.5 mJ.cm $^{-2}$, 6 ns pulse width, 0.65 Hz).

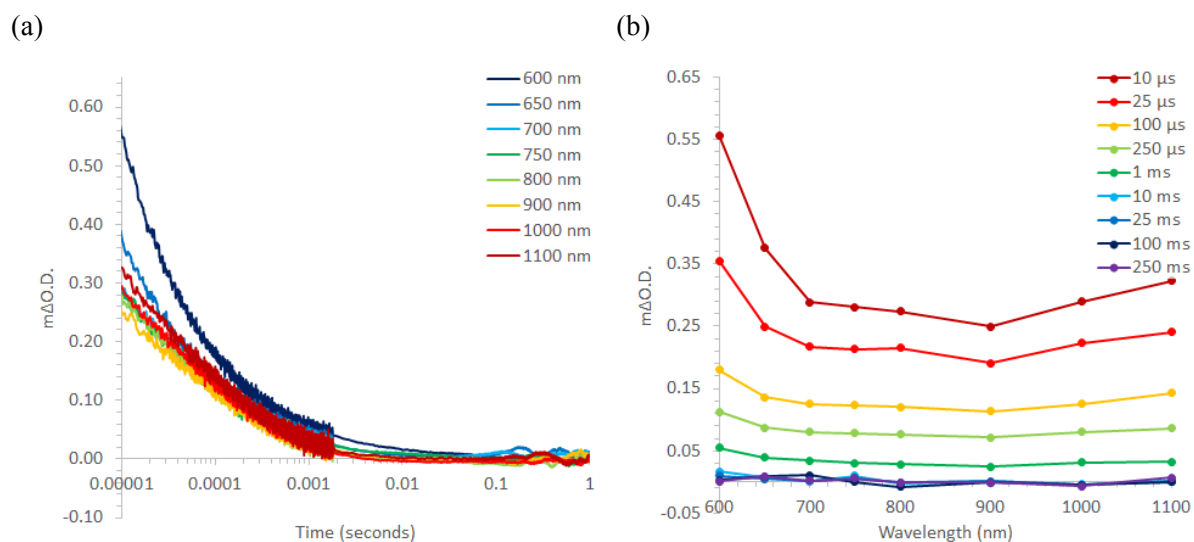


Fig. S8. (a) transient absorption decay dynamics and (b) spectral decay dynamics of an $\alpha\text{-Fe}_2\text{O}_3$ film from 10 μs after a laser pulse ($\lambda_{\text{exc}} = 500 \text{ nm}$, $\sim 0.38 \text{ mJ}\cdot\text{cm}^{-2}$, 6 ns pulse width, 0.65 Hz).

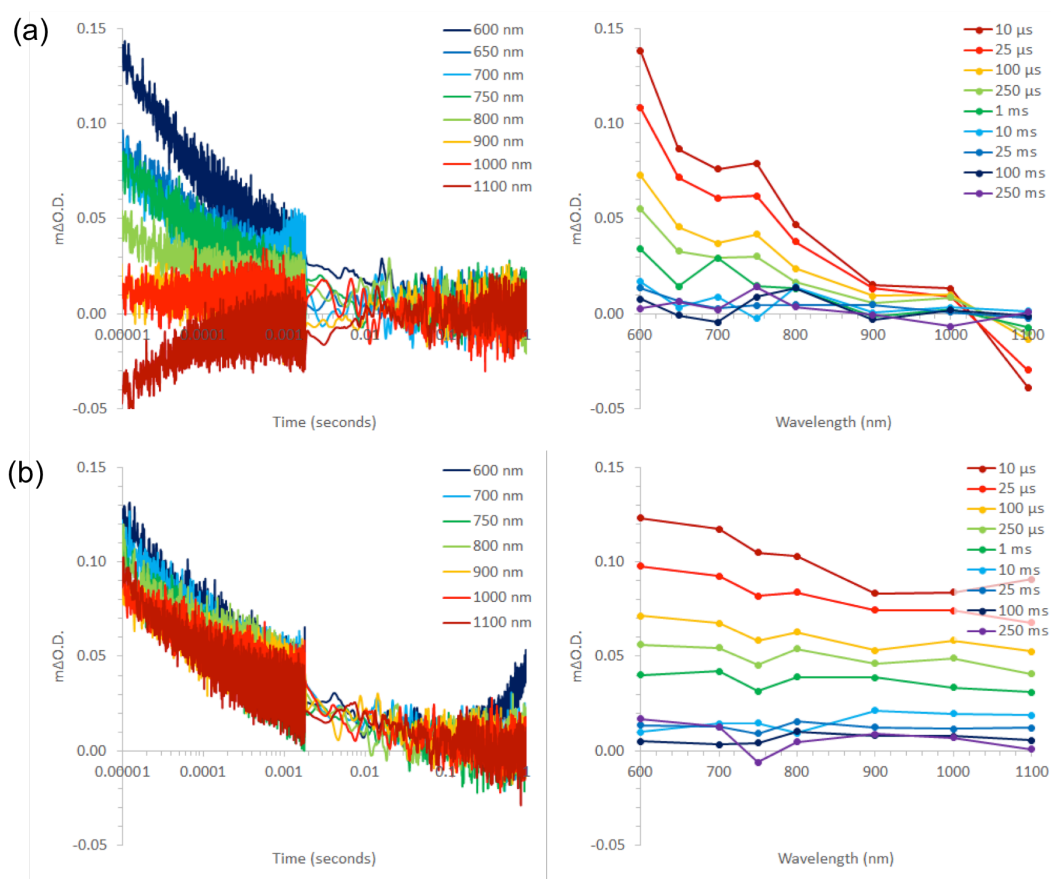


Fig. S9. (a) (left) transient absorption decay dynamics and (right) spectral decay dynamics of the $\alpha\text{-Fe}_2\text{O}_3/\text{ZnO}$ heterojunction from 10 μs after a laser pulse ($\lambda_{\text{exc}} = 355 \text{ nm}$, $\sim 0.5 \text{ mJ}\cdot\text{cm}^{-2}$, 6 ns pulse width, 0.65 Hz). The laser pump was shone onto the ZnO layer (*i.e.* front excitation). (b) (left) transient absorption decay dynamics and (right) spectral decay dynamics of the $\alpha\text{-Fe}_2\text{O}_3/\text{ZnO}$

heterojunction from 10 μs after a laser pulse ($\lambda_{\text{exc}} = 355 \text{ nm}$, $\sim 0.5 \text{ mJ}\cdot\text{cm}^{-2}$, 6 ns pulse width, 0.65 Hz). The laser pump was shone onto the $\alpha\text{-Fe}_2\text{O}_3$ layer (*i.e.* back excitation).

S7. Band alignment for the heterojunction $\alpha\text{-Fe}_2\text{O}_3/\text{ZnO}$ film

The procedure to make a band alignment was referred to Scanlon *et al.* [6]. The valence band XPS data of $\alpha\text{-Fe}_2\text{O}_3$ and ZnO (Fig. S9) were used to draw the band diagram. The extrapolation on the valence band maximum (VBM) onto x axis provides the gap energy from VBM to Fermi level energy (E_F), resulting in the value of 0.9 eV and 2.3 eV for $\alpha\text{-Fe}_2\text{O}_3$ and ZnO, respectively. As these values are relative to their own E_F , the O 1s XPS deconvoluted peaks corresponding to O^{2-} were used to locate the E_F difference between two materials. The E_F of $\alpha\text{-Fe}_2\text{O}_3$ is 0.58 eV lower than that of ZnO. To draw the band diagram of ZnO, the E_F of ZnO was firstly set at 0 eV. Then, the gap energy between VBM and E_F was used to draw the VBM energy level and the band gap energy obtained from UV-Vis data was used to draw the CBM energy level. To align the band diagram of $\alpha\text{-Fe}_2\text{O}_3$, the E_F was laid down at the energy level of 0.58 eV below that of ZnO and the full diagram was done using the same criteria for ZnO. The proposed band diagram of heterojunction films of $\alpha\text{-Fe}_2\text{O}_3/\text{ZnO}$ was shown in Fig. S10.

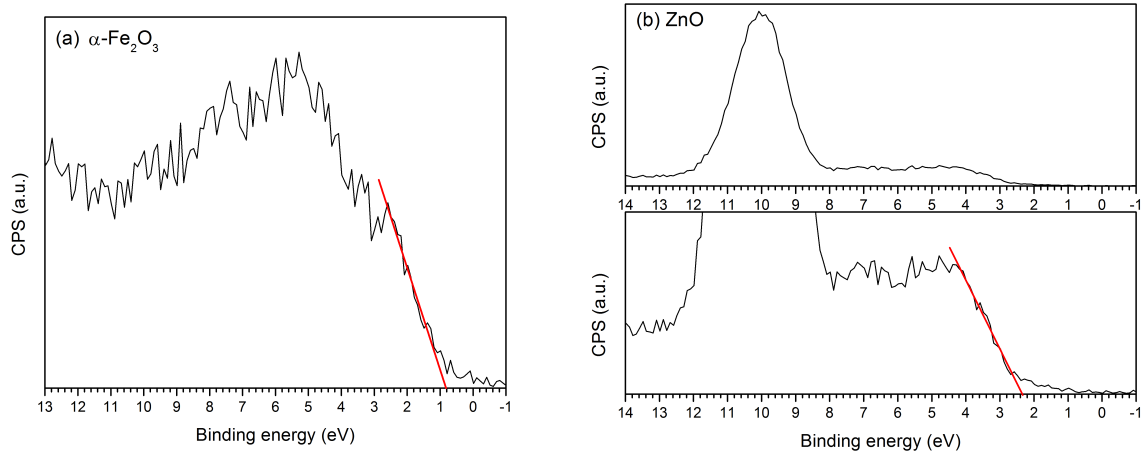


Fig. S9. The valence band XPS spectra of (a) $\alpha\text{-Fe}_2\text{O}_3$ and (b) ZnO film (the plot below showed zoom-in spectra). The extrapolation on x axis referring to the energy range from Fermi level (E_F) to valence band maximum (VBM).

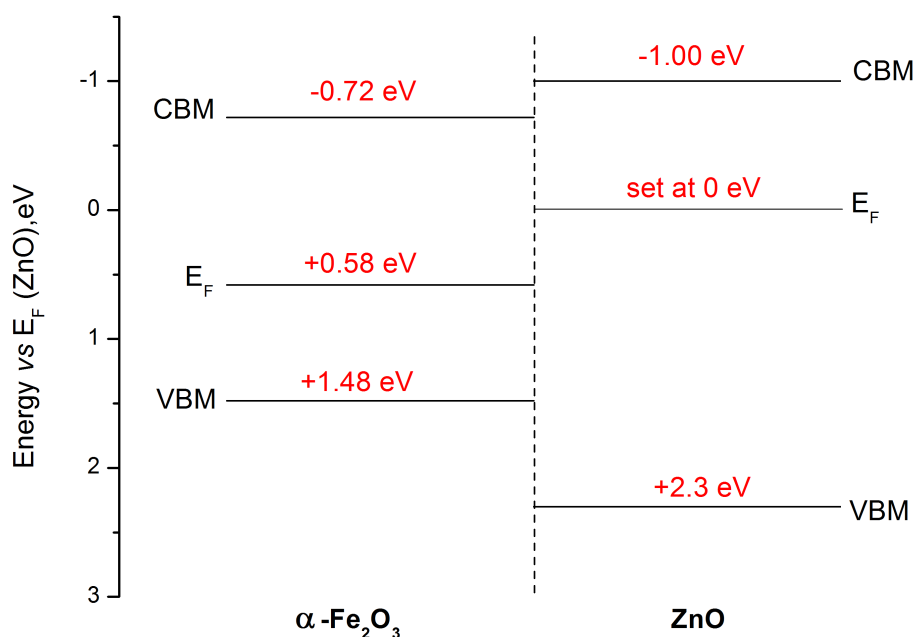


Fig. S10. The proposed band diagram of the heterojunction films of $\alpha\text{-Fe}_2\text{O}_3/\text{ZnO}$, which was aligned using the XPS data and band gap energies.

References

- [1] J. Tauc, Optical properties and electronic structure of amorphous Ge and Si, *Mater. Res. Bull.* 3 (1968) 37–46.
- [2] E.A. Davis, N.F. Mott, Conduction in non-crystalline systems V. Conductivity, optical absorption and photoconductivity in amorphous semiconductors, *Philos. Mag.* 22 (1970) 0903–0922.
- [3] P.S. Shinde, G.H. Go, W.J. Lee, Facile growth of hierarchical hematite ($\alpha\text{-Fe}_2\text{O}_3$) nanopetals on FTO by pulse reverse electrodeposition for photoelectrochemical water splitting, *J. Mater. Chem.* 22 (2012) 10469–10471.
- [4] W.Y. Liang, A.D. Yoffe, Transmission spectra of ZnO single crystals, *Phys. Rev. Lett.* 20 (1968) 59–62.
- [5] T.K. Gupta, Application of Zinc Oxide Varistors, *J. Am. Ceram. Soc.* 73 (1990) 1817–1840.
- [6] D.O. Scanlon, C.W. Dunnill, J. Buckeridge, S.A. Shevlin, A.J. Logsdail, S.M. Woodley, C.R.A. Catlow, M.J. Powell, R.G. Palgrave, I.P. Parkin, G.W. Watson, T.W. Keal, P. Sherwood, A. Walsh, A.A. Sokol, Band alignment of rutile and anatase TiO_2 , *Nat. Mater.* 12 (2013) 798–801.